Article

Proteomic Analysis of Anti-Aging Effects of *Dendrobium Nobile Lindl.* Alkaloids in Aging-Accelerated SAMP8 Alzheimer's Mice

Bo Liu*, Ling-li Lv, Ping Liu, Yun-yan Xu, Jie Liu, Jing-Shan Shi

Key Lab for Basic Pharmacology of Ministry of Education, Zunyi Medical University, Zunyi, 563000, China. 463848472@qq.com (B.L.); 1982711310@qq.com (L-L.L.); lpliuing@163.com (P.L.); 624351565@qq.com (Y-Y.X.); JieLiu@zmu.edu.cn (J.L.); shijs@zmu.edu.cn (J-S.S.);
* Correspondence: yaoliliubo@zmu.edu.cn; Jie@liuonline.com.)

Abstract: Senescence-accelerated mouse prone 8 (SAMP8) mice exhibit cognitive defects and neuron loss with aging, and are used to study anti-aging effects of *Dendrobium nobile* alkaloids (DNLA). SAMP8 mice were orally given DNLA from ages 6 to 10 months. At 10 months of age, behavioral tests and neuron damage were evaluated. Protein was extracted and subjected to phosphorylated proteomic analysis. The cognitive deficits and neuron loss in hippocampus and cortex of aged SAMP8 mice were improved by DNLA. Hippocampal proteomic analysis showed differentially expressed protein/genes in SAMP8 compared to age-matched senescence-accelerated resistant mice, including altered tubulin binding, microtubule binding, etc. via Gene Oncology. KEGG revealed endocytosis, mRNA surveillance, tight junction, protein processing in endoplasmic reticulum, aldosterone synthesis and secretion, and glucagon signaling pathway changes. Upregulated protein/genes in the hippocampus of SAMP8 mice, such as Lmtk3, Usp10, Dzip1, Csnk2b, and Rtn1, were attenuated by DNLA; whereas downregulated protein/genes, such as Kctd16, Psd3, Bsn, Atxn2l, and Kif1a, were rescued by DNLA. The aberrant protein/gene expressions of SAMP8 mice were correlated with transcriptome changes of Alzheimer's disease in the GEO database, and were attenuated by DNLA. Thus, DNLA improved cognitive dysfunction and ameliorated neuronal injury in aged SAMP8 mice, and attenuated aberrant protein/gene expressions.

Keywords: SAMP8 and SAMR1 mice; DNLA (*Dendrobium nobile* Lindl. alkaloids); Cognition; Nissl staining; Phosphorylated Proteomics; Bioinformatics

1. Introduction

The senescence-accelerated mouse model 8 (SAMP8) mice exhibit a number of clinical manifestations of Alzheimer's disease (AD), such as cognitive defects and neuron loss, and have been used as an animal model for age-related AD research [1-4]. Cognitive deficits deteriorate in SAMP8 mice with aging compared to age-matched senescence-accelerated resistant mice 1 (SAMR1) mice [3]. Thus, aged SAMP8 mice and age-matched SAMR1 mice are commonly used to study anti-aging mechanisms and anti-AD remedies [4].

Dendrobium species, a class of famous Chinese medicines, have been used for age-related diseases [5], including Alzheimer's disease (AD) to improve the quality of life of the elderly. DNLA (*Dendrobium nobile Lindl.* alkaloids) has been demonstrated to alleviate age-related disorders [6] and have anti-AD effects [7]. Our previous studies have indicated that DNLA reduces hippocampal neuron loss and synaptic dysfunction induced by $A\beta_{25-35}$ in rats [8], in Aβ damaged hippocampal and cortical primary neurons [9-11]. Moreover, DNLA also improved the cognitive deficits in multiple Alzheimer's disease models, including the APP/PS1 double transgenic mice [12], lipopolysaccharide-induced dementia rats [13], and also in SAMP8 mice [14, 15].

 doi:10.20944/preprints202212.0313.v1

To further explore the molecular mechanisms by which DNLA improves cognitive defects in aged SAMP8 mice, the current study used phosphorylated proteomic approach to examine hippocampal proteomic changes, a brain region responsive for cognitive function, with or without DNLA treatment for 4 months. The Y-maze and Open-field tests as well as Nissl strain were performed in conjunction with phosphorylated proteomic analysis, followed by compressive bioinformatics analysis and correlation analysis with transcriptome changes of AD in accessible GEO database in the National Library of Medicine. The results clearly demonstrated the beneficial effects of DNLA against aged SAMP8 mice and identified several novel molecular targets for future studies.

2. Materials and Methods

2.1. Animals

Male SAMP8 and SAMR1 mice (2-month-old) were purchased from Peking University (SCXK2016-0010) and maintained in accredited (SYXK 2014-003) SPF-grade animal room at Key Lab of Basic pharmacology of Zunyi Medical University. Drinking water and rodent chow were provided ad libitum with 50% humidity, 22 – 24 °C, and 8:00 am-8:00 pm light/dark cycle. Animal experiment procedures complied with the Chinese Animal Care and Use Guidelines and the study protocol was approved by Institutional Animal Use and Care Committee with ethical number of [2020]2-142.

2.2. Drugs

DNLA was extracted from Dendrobium nobile Lindl., which has been verified in http://www.theplantlist.org. Dendrobium nobile Lindl. was from Xintian Pharmaceutical Ltd. (Chishui, Guizhou, China). The alkaloids were extracted and purified in our laboratory. The DNLA content was 79.8 % as detected by LC-MS, including Dendrobine-N-oxide, Dendrobine, Dendroxine, Nobilonine, 6-Hydroxynobilonine and 13-Hydroxy-14-oxodendrobine as previously described[8, 9, 6]. Ultimately, DNLA were dissolved in Tween 80 (1%) for oral administration.

2.3. Experimental design

Mice were randomly grouped to SAMR1 (genetic Control), SAMP8 (Model Control), SAMP8 plus DNLA 20 mg/kg, and SAMP8 plus DNLA 40 mg/kg groups. The dose selection of DNLA was chosen from our previous publications [14, 15]. DNLA treatment lasted for 4 months staring at the 6-momth-old of age, and Controls received normal saline. Behavioral tests were performed at 10-month of age. Mice were then euthanatized, and brains of three mice in each group were fixed for Nissl staining, and the hippocampus of another three mice were frozen at -80 °C for phosphorylated proteomic analysis.

2.4. Behavioral tests

The learning and memory ability of aged rats was tested by Y maze free alternating experiment with camera recording system (Topscan, CleverSys, Inc., Reston, VA, USA) [16]. The mice were free to explore the three arms of Y maze for 10 minutes and the order of arm entries and corrected entries were recorded as described previously [14].

The locomotor activity was tested by Open-field experiment [17]. Total distance the mice traveled between the central and peripheral regions were recorded as described previously [15].

2.5. Nissl staining

Paraformaldehyde (4%) was used to fix the brain. Then the mouse brains were embedded in paraffin, and cut into 5 μm thick sections for Nissl staining. The paraffin-embedded sections were deparaffinized and rehydrated in xylene and gradient alcohol solutions, and washed in PBS. Nissl staining solution (Solarbio, Beijing, China) was used to stain Nissl bodies. Nissl bodies in the hippocampal CA1 region and prefrontal cortex

Preprints (www.preprints.org) | NOT PEER-REVIEWED | Posted: 19 December 2022 doi:10.20944/preprints202212.0313.v1

were examined under light microscope (Leica Microsystems Ltd., Wetzlar, Germany) and quantified with Image J as described previously [14, 15].

2.6. Protein phosphorylation analysis

Since DNLA 20 mg/kg was effective as DNLA 40 mg/kg, the DNLA 20 mg/kg group was selected for proteomic analysis. Cold homogenization buffer (8 M urea in PBS, 1 × protease and phosphatase inhibitor G) was used to lyse the hippocampal tissues, followed by sonication for protein extraction. Lysates were centrifuged (12000 g, 4 °C, 20 min) and protein content in the supernatant was determined by BCA protein assay kit (Thermo Fisher, Durham, NC, USA). Proteins were incubated with 10 mM dithiothreitol (30 min, 55 °C), then incubated with iodoacetamide (25 mM, 1 h) and then diluted with PBS to reach a final urea concentration with 1.0 M and digested with trypsin (1:100 w/w for 14 h at 37 °C). After digestion, peptides were adjusted to acidic pH 1-2 with 1% formic acid (FA) and centrifuged (12000 g, 15 min) to collect the supernatant, and then desalted with an inverting column (Oasis HLB, Waters, USA), dried in a vacuum centrifuge and dissolved in triethylammonium bicarbonate buffer (TEAB, 200 mM, pH 8.5) for TiO2 enrichment or Tandem Mass Tag (TMT) labeling [18].

2.7. GO and KEGG analysis

The Gene Ontology (GO) and Kyoto Encyclopedia of Genes and Genomes (KEGG) were performed with DAVID online database (https://david.ncifcrf.gov/). GO and KEGG pathway enrichment analysis were used to reflect the biological process, molecular function, cellular component, and enriched pathways of aged SAMP8 mouse brain. Results were displayed in a bubble chart, the smaller the p value the higher the degree of enrichment; the larger the count the more genes are enriched.

2.8. Differentially expressed protein/genes analysis

The criteria for differentially expressed protein/genes were set at $p < 0.05$ and > 1.2-fold change, as compared to SAMR1 control mice. Hierarchical complete linkage was performed with Gene Cluster version 3.0 (https://cluster 2. software.informer.com/3.0/), and visualized with TreeView version 1.6 (https://treeview.software.informer.com/1.6/) as 2D-heatmap.

2.9. Correlation Engine analysis with the GEO database

Differentially expressed protein/genes from SAMP8 mice vs SAMR1 control mice were imported into Illumina BaseSpace Correlation Engine (BSCE) for curated studies with biosets in Gene Expression Omnibus (GEO) database, using -log(p-value) methods [19]. The larger the -log(p-value), the higher degree of similarity.

2.10. Statistical analysis

Phosphorylated proteomic data were initially analyzed by the company (Swiss PRO Bio-tech Co., LTD, Shanghai, China) with the criteria of $p < 0.05$ and fold change > 1.2, followed by bioinformatics analysis. The behavioral tests and Nissl counting data were analyzed by statistics software SPSS 20.0. The one-way analysis of variance (ANOVA) and Bonferroni test were used to analyze the behavioral tests and Nissl counting. The values were expressed as mean ± SD. The significant criteria was set at $p < 0.05$.

3. Results

3.1. DNLA improved cognitive functions

The experimental design is shown below (Fig. 1A). The short-term spatial working memory was evaluated by Y-maze spontaneous alternation test (Fig. 1B) and locomotor activity by Open-field test (Fig. 1C). Compared with the SAMR1 mice, the short-term spa-

Preprints (www.preprints.org) | NOT PEER-REVIEWED | Posted: 19 December 2022 doi:10.20944/preprints202212.0313.v1

tial working memory of 10-month-old SAMP8 mice decreased significantly ($p < 0.05$). Fortunately, the short-term spatial working memory was obviously improved after 4 months of DNLA treatment (20 and 40 mg/kg) (Fig. 1B). The result of Open-field test showed that total travel distance between the central region and peripheral region of 10-month-old SAMP8 mice was significantly decreased compared with SAMR1 mice. After continuous 4 months treatment with DNLA (20 and 40 mg/kg), the decreases in total distance of SAMP8 mice was reversed.

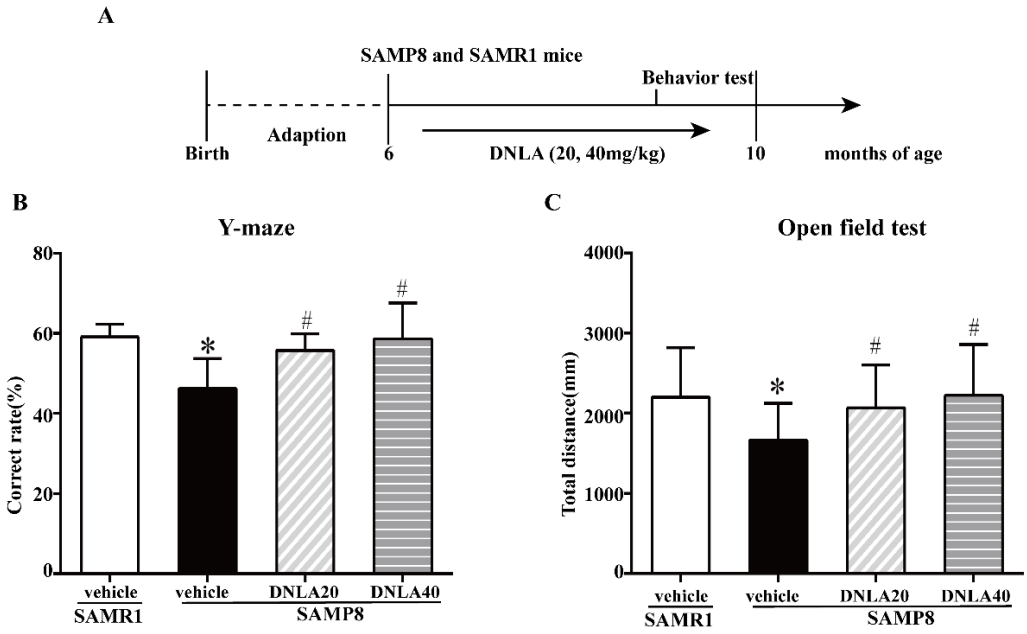

Figure 1. The effects of DNLA on spatial working memory and locomotor impairment in SAMP8 mice. A. Schematic diagram of experimental progress. B. The correct rate of Y-maze spontaneous alternation. C. The total distance traveled by the mouse from the central and peripheral regions of Open-field test Data are Mean ± SD of n=10, *$p < 0.05$ vs SAMR1 mice, #$p < 0.05$ vs SAMP8 mice.

3.2. DNLA ameliorated neuron lesions in the brain of SAMP8 mice

The morphology of neurons in the hippocampal CA1 region and prefrontal cortex were examined by Nissl staining. In SAMR1 control mice, granule neurons exhibited round nuclei, which were located in the center of the perikaryon and surrounded by a pale cytoplasm. A significant loss of Nissl-stained neurons and vacuoles were observed in the 10-month-old SAMP8 mice. Luckily, Nissl-stained neurons in the CA1 region of hippocampus and prefrontal cortex were increased after four months of treatment with two doses of DNLA (20 and 40 mg/kg), compared with those in the SAMP8 group ($p < 0.05$).

Preprints (www.preprints.org) | NOT PEER-REVIEWED | Posted: 19 December 2022 doi:10.20944/preprints202212.0313.v1

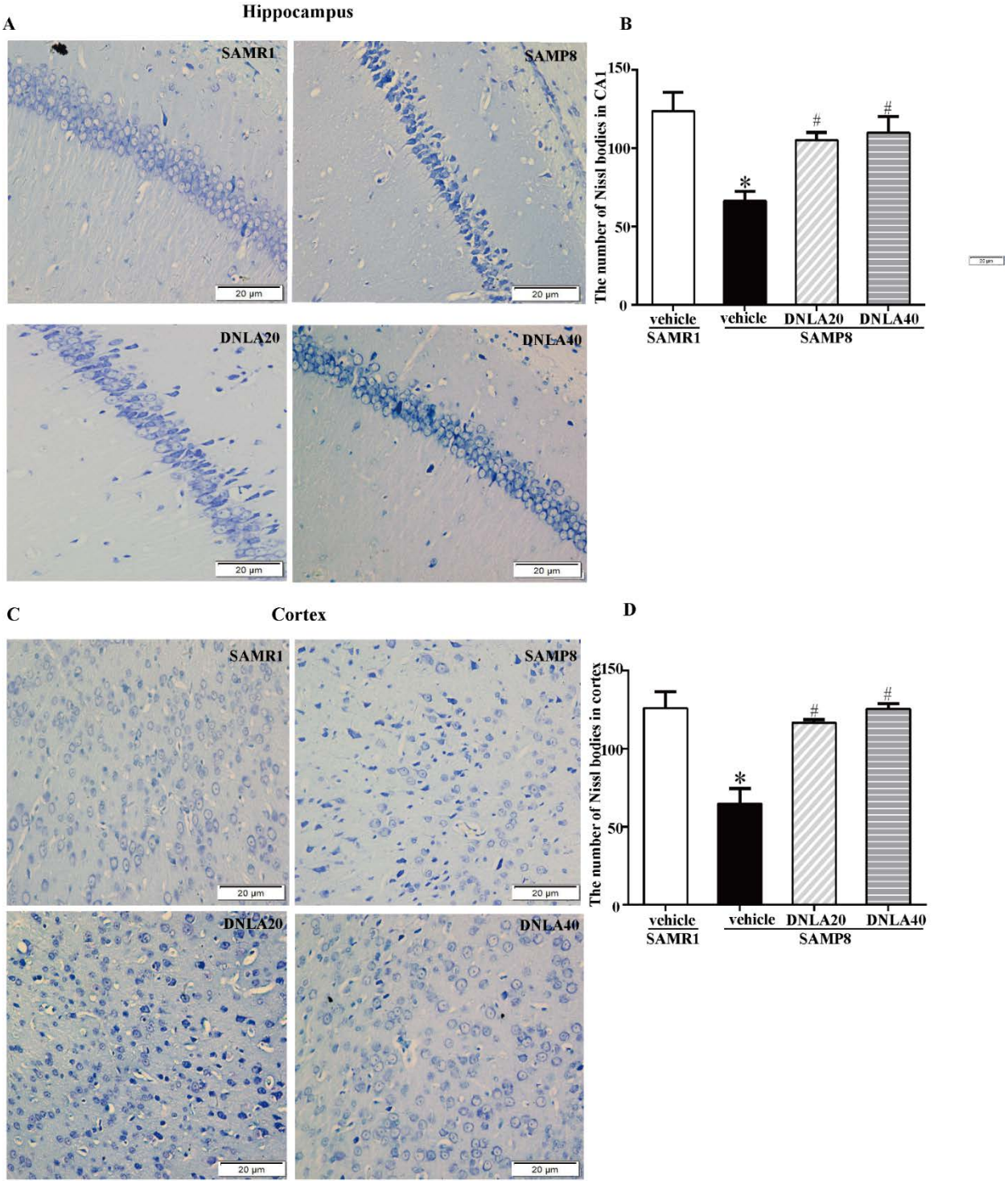

Figure 2. The effects of DNLA on Nissl staining of the hippocampus and prefrontal cortex of SAMP8 mice. A. Nissl bodies in the hippocampal CA1 region (magnification 200×, scale bar=50 μm); B. Quantitation of Nissl bodies in the hippocampal CA1 region; C. Nissl bodies in the prefrontal cortex (magnification 200×, scale bar=50 μm); D. Quantitation of Nissl bodies in the prefrontal cortex. Data are Mean ± SD of n=3, *p < 0.05 vs SAMR1 mice, #p < 0.05 vs SAMP8 mice.

3.3. DNLA alleviated differentially expressed protein/genes.

Proteomics data were obtained by preprocessing LC-MS/MS based on ion intensity and spectral count. Volcano plot displays differentially expressed phosphorylated proteins in the hippocampus of SAMR1, SAMP8, and SAMP8 mice received DNLA (20 mg/kg) treatment, respectively (Figure 3A). In SAMP8 vs SAMR1, there were 14395 reads,

Preprints (www.preprints.org) | NOT PEER-REVIEWED | Posted: 19 December 2022 doi:10.20944/preprints202212.0313.v1

8853 quant protein/genes, 2978 after A-Score filter, and 196 differentially expressed protein/genes ($p < 0.05$ and 1.2 fold cut) were finally identified. In SAMP8+DNLA vs SAMR1, there were 13652 reads, 6859 quant protein/genes, 3098 after A-Score filter, and 242 differentially expressed protein/genes were finally identified. In SAMP8+DNLA vs SAMP8, there were 13289 reads, 8123 quant protein/genes, 3209 after A-Score filter, and 38 differentially expressed protein/genes were finally identified. Compared with SAMR1 control group, SAMP8 had 46 phosphorylated proteins upregulated and 150 phosphorylated proteins downregulated (Figure 3B). In the SAMP8+DNLA-treated mice, 55 phosphorylated proteins were upregulated and 187 phosphorylated proteins were downregulated as compared to SAMR1 control mice. When SAMP8+DNLA group compared to SAMP8 group, 13 increased and 25 decreased.

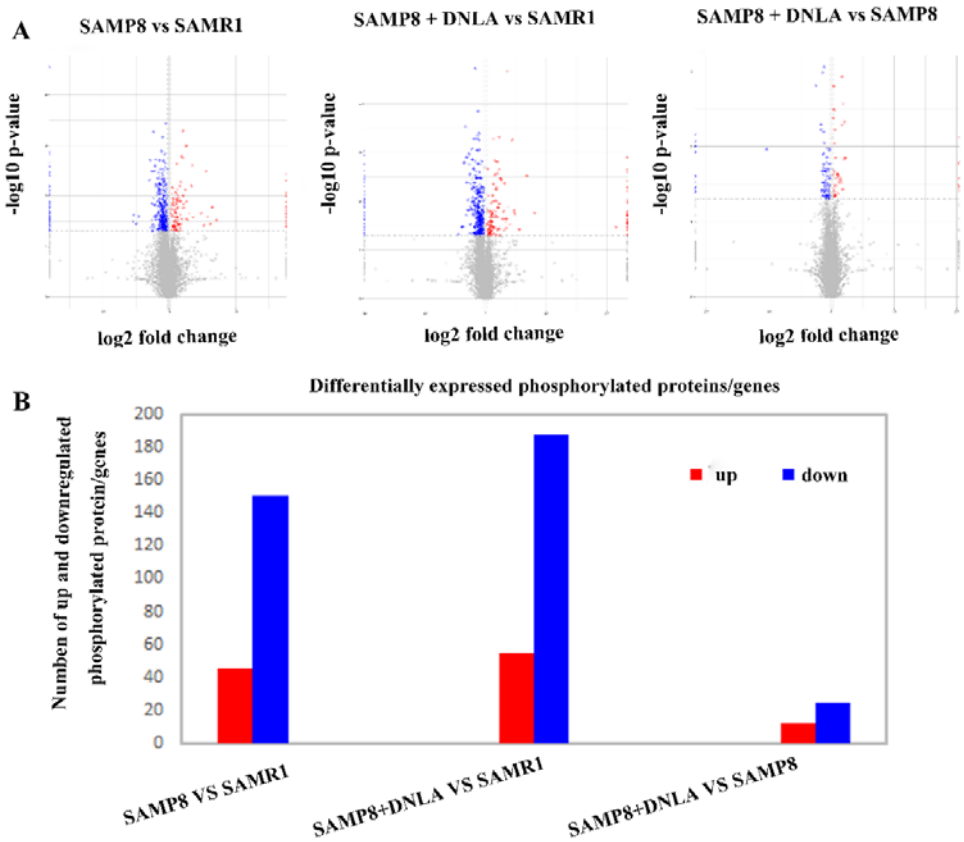

Figure 3. Differentially expressed phosphorylated proteins following treatment with DNLA in hippocampus of SAMP8 mice. A. Volcano scatter plots of log2 fold change (X-axis) against -log2 fold change (Y-axis) of all quantified phosphorylated proteins. Upregulated phosphorylated proteins are colored red, and downregulated proteins are colored blue. The differentially expressed phosphorylated proteins among groups could be visualized. B. Differentially expressed phosphorylated proteins compared to SAMR1 control, and DNLA treatment compared to SAMP8 mice.

3.4. GO and KEGG analysis

Gene Ontology (GO) and Kyoto Encyclopedia of Genes and Genomes database (KEGG) analysis were conducted to better understand the biological function of differentially expressed phosphorylated proteins/genes in SAMP8 mice vs SAMAR1 mice. The top 20 of GO enriched biological processes (Fig. 4A) indicated that the biological processes of the phosphorylated proteins/genes were mainly involved in tubulin binding, microtubule binding and actin binding etc. The KEGG enriched signaling pathways involved in

Preprints (www.preprints.org) | NOT PEER-REVIEWED | Posted: 19 December 2022 doi:10.20944/preprints202212.0313.v1

endocytosis, mRNA surveillance pathway, tight junction, and protein processing in endoplasmic reticulum, aldosterone synthesis and secretion, and glucagon signaling pathway (Fig. 4B).

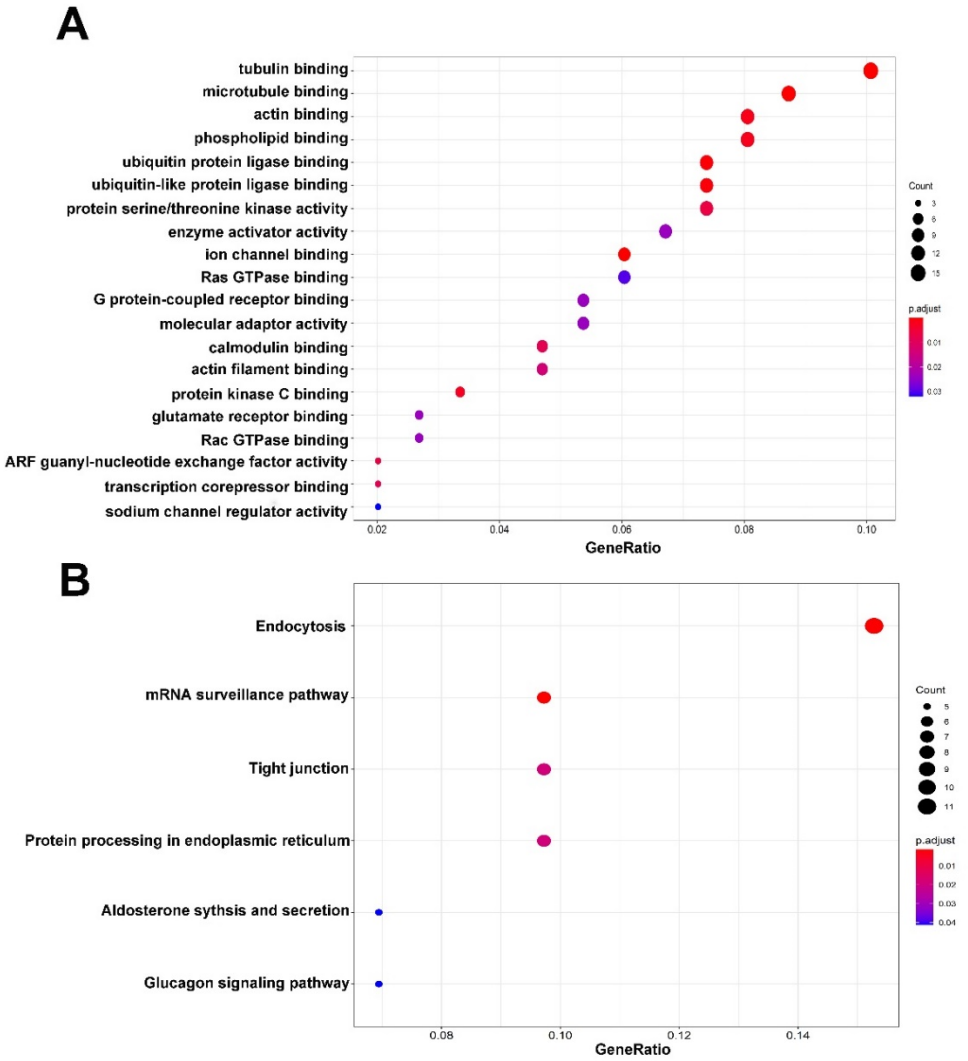

Figure 4. GO and KEGG analysis. A. GO analysis shows biological processes. B. KEGG shows signaling pathways. The size of the points in the figure represents the number of annotated phosphorylated proteins/genes, the color of the points in the figure represents the enrichment significance of the functional pathway with GeneRatio.

3.5. Differentially phosphorylated proteins/genes analysis

Differentially expressed phosphorylated protein/genes (DEP/DEGs) were analyzed under the criteria of $p < 0.05$, 1.2-fold cut. Figure 5 shows 2-D clustering heatmap with up-regulation in red and down-regulation in blue. Some selected clusters were arrow indicated for examples. The entire 298 list of 2-D clustering analysis with gene name annotation is provided as Supplementary Table 1.

Preprints (www.preprints.org) | NOT PEER-REVIEWED | Posted: 19 December 2022 doi:10.20944/preprints202212.0313.v1

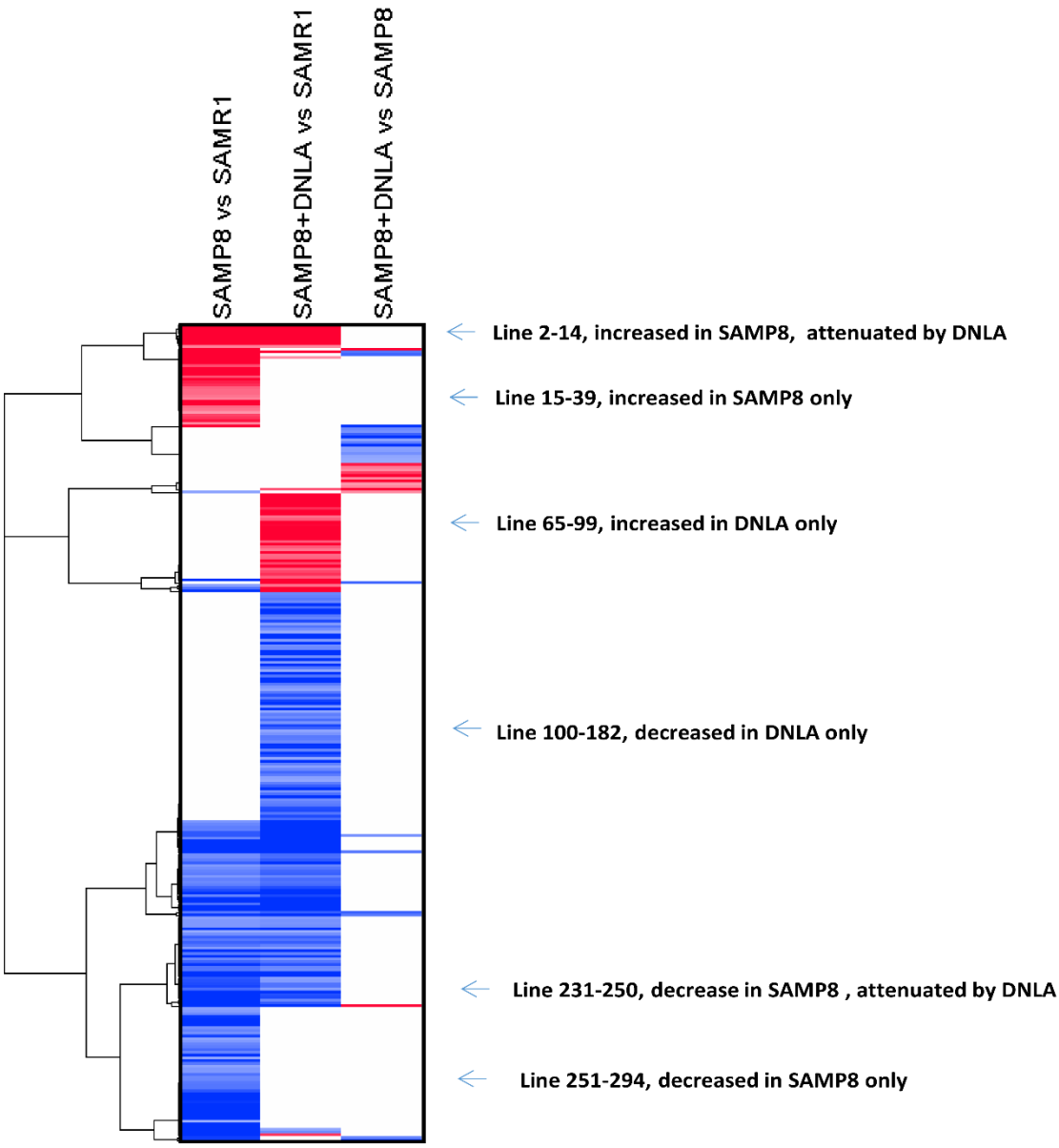

Figure 5. Two-dimensional clustering analysis. The differentially expressed phosphorylated proteins/genes in SAMP8 vs SAMR1, SAMP8+DNLA vs SAMR1, SAMP8+DNLA vs SAMP8 groups were clustered. Red indicates upregulation and blue indicates downregulation. Some clusters unique to SAMP8, and/or SAMP8+DNLA were indicated by arrows.

3.6. Heatmap of top 30 altered phosphorylated protein/genes

The selected 30 differentially expressed protein/genes are shown in Figure 6 in a fashion of "Gene_Protein_Peptide". It is obvious that DNLA treatment attenuated aberrant protein/gene expressions in SAMP8 mice. Compared to SAMR1 control, overexpressions of Lmtk3 (140-fold), Dzip1 (100-fold), Csnk2b (70-90-fold), and Rnt1 (60-fold) in SAMP8 mice were not seen after DNLA treatment, and overexpressions of Usp10 (139 to 110), Stmn1 (27 to 21), and Ankrd34a (10.8 to 8.7) were attenuated by DNLA. The dramatic downregulation of Kctd16 (-45-fold), Psd3 (-40-fold), and Bsn (-24-fold) in SAMP8 mice were not seen after DNLA treatment. The significant downregulation of Atxn2l, Kif1a, Kif21a, Srrm2, Gpsm1, Nudc, and Mbp (-6 to -7 fold) in SAMP8 mice were prevented by DNLA. It should be mentioned that there were two peptides of Csnk2b, and both were increased 70-90 fold; and there were two peptides of Tbc1d24, one was increased 8.2-fold, and another was decreased -10-fold. When SAMP8+DNLA was compared with SAMP8,

Preprints (www.preprints.org) | NOT PEER-REVIEWED | Posted: 19 December 2022 doi:10.20944/preprints202212.0313.v1

only 3 decreased, opposite to SAMP8 (Lmtk3, -2 fold; Dzip, -2.7 fold; Herc1, -5.2 fold) and one slightly increased (Rtn1, 7 fold).

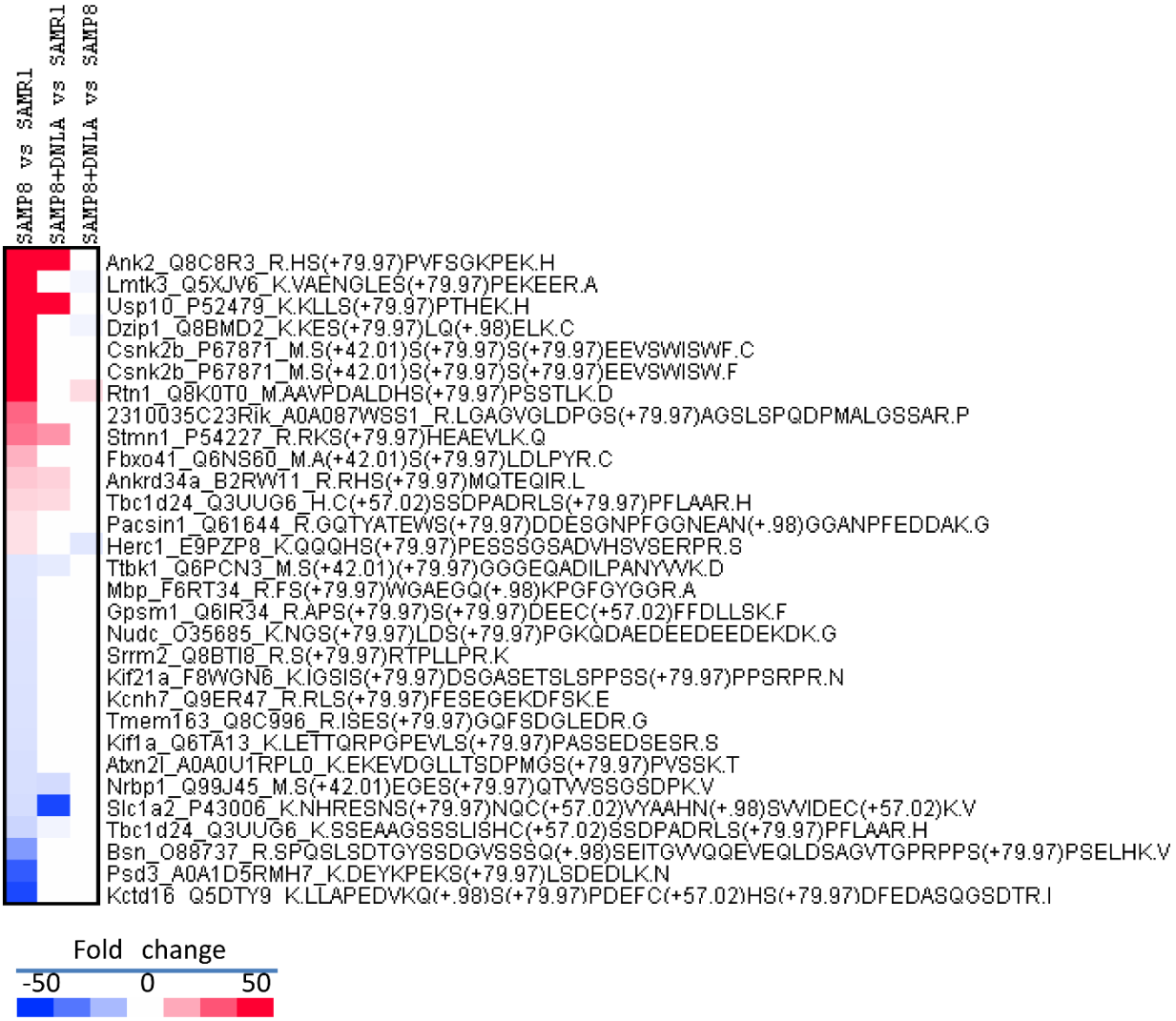

Figure 6. Heatmap of top 30 altered phosphorylated protein/genes. The differentially expressed protein/genes among SAMP8 vs SAMR1, SAMP8+DNLA vs SAMR1, SAMP8+DNLA vs SAMP8 groups in a fashion of "Gene_Protein_Peptide". Based on fold-changes with upregulation in red and downregulation in blue.

3.7. Correlation with the GEO database

The DEP/DEGs were imported into Illumina BaseSpace Correlation Engine (BSCE) for curated studies with the GEO database. The biosets were filtered by "rat, mice and human", "RNA expression" and "Alzheimer's disease", and the -log (p-values) were calculated to compare with the GEO database. The 10 GSE databases related to Alzheimer's disease were selected based on SAMP8 vs Controls (Figure 7). DNLA treatment attenuated the –log(p values) (lighter color in the heatmap), suggesting that DNLA ameliorate the aberrant gene expression from aged SAMP8 mice.

Preprints (www.preprints.org) | NOT PEER-REVIEWED | Posted: 19 December 2022 doi:10.20944/preprints202212.0313.v1

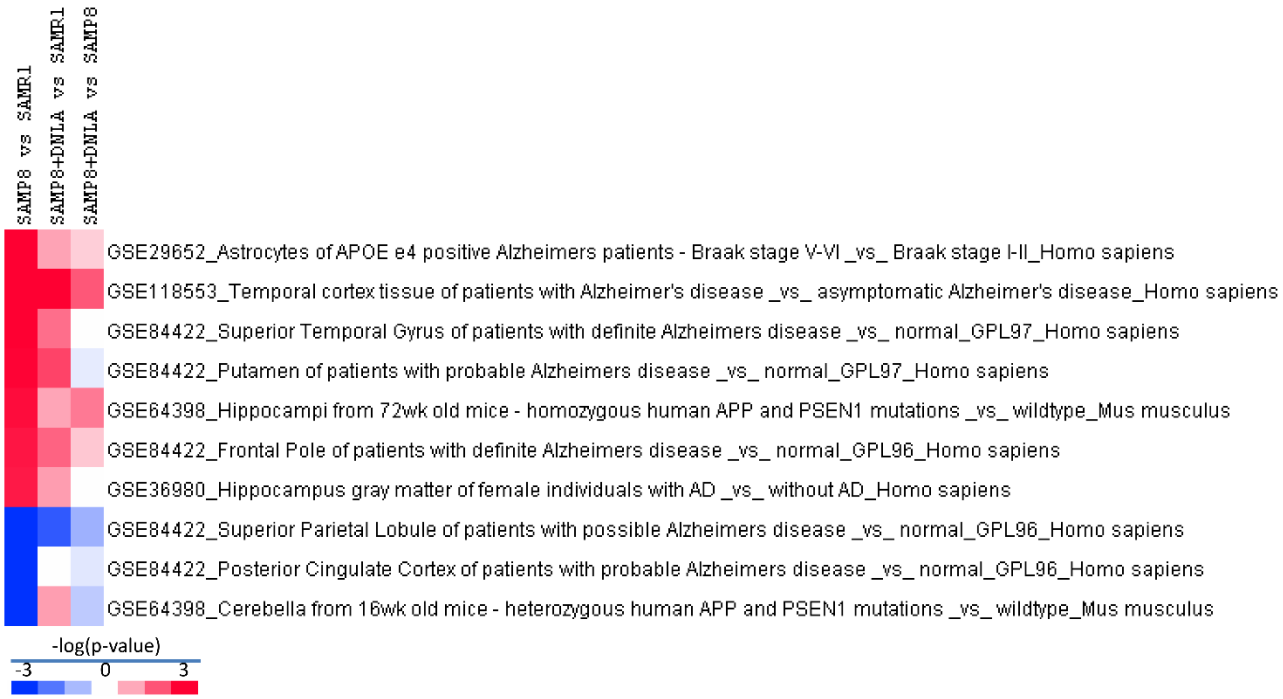

Figure 7. Correlation with the GEO database analysis. The differentially expressed protein/genes among SAMP8 vs SAMR1, SAMP8+DNLA vs SAMR1, SAMP8+DNLA vs SAMP8 groups were imported into Illumina Correlation Engine to compare the GEO database using –log(p-value) with upregulation in red and downregulation in blue. The correlations were in the format of the GSE number_Study name in the GEO database.

4. Discussion

The present study clearly showed that 4 months of DNLA treatment effectively ameliorated age-accelerated cognitive impairment and neuron loss in aged SAMP8 mice. Phosphorylated proteomics revealed differentially expressed protein/genes in the hippocampus of SAMP8 mice. GO and KEGG enrichments revealed the major molecular events and signaling pathways. DNLA ameliorated aberrant protein/gene expression patterns as evidenced by 2-dimentional clustering analysis and by top 30 altered protein/gene expression comparisons. Proteomics changes in the hippocampus of SAMP8 mice were correlated with transcriptome changes of Alzheimer's disease in the GEO database, such correlations (–log (p-values) were attenuated by DNLA. Overall, this study demonstrated neuroprotective effects of DNLA, but also revealed novel molecular targets through proteomic analysis.

4.1. DNLA improved behavioral impairments and neuron damage in SAMP8 mice

Age-related deficits in cognitive function are the major manifestations in aged SAMP8 mice [4], as evidenced by Y-maze test [14] and Open-field test [15]. DNLA treatment for 4 months clearly increased the correctness of spontaneous alternation in Y-maze and the travel distance and central entry in Open-field tests. DNLA also improved rotarod activity in aged SAMP8 mice [15] and improved learning and memory of APP/PS1 mice in Morris water maze tests [12]. Thus, DNLA could improve age-related cognitive impairment.

Hippocampal CA1 region is important for cognitive functions，neuronal loss and morphological changes occur in the hippocampus and prefrontal cortex of SAMP8 mice [20]. Neuron loss in hippocampus CA1 region and cortex are evident in aged SAMP8 mice, causing impaired learning and memory [21]. This study confirmed that aged SAMP8 mice had neuron loss in these brain regions, which were ameliorated after DNLA treatment,

Preprints (www.preprints.org) | NOT PEER-REVIEWED | Posted: 19 December 2022 doi:10.20944/preprints202212.0313.v1

confirming the beneficial effects of DNLA against aging-accelerated neuronal degeneration in SAMP8 mice [14, 15].

4.2. Aged SAMP8 mouse hippocampus showed differential protein/gene expression

Compared to SAMR1 mice, the hippocampus of SAMP8 mice had 196 differentially expressed protein/genes, and the top GO enriched biological processes and KEGG enriched pathways were identified as the first step to analyze differentially expressed protein/genes, a strategy used in our recent publication [22]. Using cDNA microarray, the differentially expressed genes were identified in aged SAMP8 mice as compared to 2 month-old SAMP8 mice and SAMR1 mice [23]. A number of aberrant gene and protein expressions in the brain of SAMP8 mice have been reviewed [1], and the current study further outlined the 2D-cluster to help our understanding of the differences among SAMP8, SAMR1, and DNLA treatment groups. The top 30 protein/genes were selected for discussion below.

4.3. Upregulated protein/genes in aged SAMP8 mice and effects of DNLA

Based on SAMP8 vs SAMAR1 control, there were 14 upregulated protein/genes (6-100+ fold), which were alleviated by 4-month of DNLA treatment. The LMTK family of kinases (Lmtk1-3) is important in cell physiology and pathogenesis, and imbalanced LMTK levels are implicated in neurodegenerative diseases [24]. DNLA prevented the upregulation of Lmtk3 in SAMP8 mice. The ubiquitin-specific protease 10 (Usp10) is a critical factor for the formation of Tau/TIA1/USP10-positive SGs in Alzheimer's brain [25]. Usp10 was increased 140-fold in the SAMP8 mice, which was attenuated by DNLA to 110-fold. Increased expression of dZip1 (Zn transporter) was found in the brains of $A\beta_{42}$-expressing flies, and genetic inhibition dZip1 ameliorated Aβ pathology and improved cognitive performance [26]. Fortunately, the upregulation of dZip1 was abolished by DNLA. Casein kinase 2 beta (Csnk2b) is identified as a new gene for neurodevelopmental disorders [27]. Two peptides of Csnk2b were increased 70-90 fold in the hippocampus of SAMP8 mice, and DNLA prevented such increases. Reticulon protein 1 (Rtn1) is localized in dendrites and plays a role in the formation of senile plaques in Alzheimer's brains [28], and the upregulation of Rtn1 was suppressed by DNLA. Stathmin1 (Stmn1) expression is associated with aging and Alzheimer's disease [29]. Overexpression of Stmn1 (27-fold) was attenuated by DNLA (20-fold). F-box protein 41 (Fbxo41) targets centrosomes to regulate neuronal cilia structure and signaling capacity playing roles in brain development and diseases [30]. Overexpression of Fbxo41 was prevented by DNLA. TBC1 domain family member 24 (Tdc1d24) regulates the maintenance of excitatory synapses and animal behaviors [31]. In this study one peptide of Tdc1d24 increased 8-fold, which was attenuated by DNLA to 7-fold; and another peptide was decreased -10-fold that was ameliorated to -2.3-fold by DNLA. Protein kinase C and casein kinase substrate in neurons 1 (Pacsin1) regulates synapse function and interacts with microtubule-associated protein Tau in neurodegenerative diseases [32]. Overexpression of Pacsin1 (5.9-fold) was prevented by DNLA. HECT and RLD domain containing E3 ubiquitin protein ligase family member 1 (Herc1) is required for hippocampal learning and memory by regulating synaptic activity [33]. DNLA inhibited the upregulation of Herc1. Overall, these overexpressed protein/genes in SAMP8 mice were prevented or attenuated following DNLA treatment.

4.4. Downregulated protein/genes in aged SAMP8 mice and effects of DNLA

There were 16 downregulated protein/genes (-6 to -45 fold) in SAMP8 mouse brain. The dramatic downregulations were potassium channel tetramerization domain containing 16 (Kctd16, -45-fold), pleckstrin and Sec7 domain containing 3 (Psd3, -40-fold), and bassoon presynaptic cytomatrix protein (Bsn, -24-fold). Kctd16 interacts with amyloid β precursor protein in Alzheimer's disease [34]; Psd3 is identified as one of hippocampal genes for amyloid-beta formation in Alzheimer's disease [35]; Bsn exhibits an early-up,

 doi:10.20944/preprints202212.0313.v1

late-down expression pattern at pathologic stages of Alzheimer's disease [36]. DNLA prevented the downregulation of these protein/genes. Ataxin 2 like (Atxn2l) deletion resulted in embryonic death, and implicated in neurodegenerative diseases [37]. Atxn2l was downregulated -7.5-fold, but was prevented by DNLA. Kinesin family member 1A (Kif1a) and kinesin family member 21A (Kif21a) are involved in hippocampal synaptogenesis, axonal transport and selective somatodendritic endocytosis and learning enhancement [38, 39]. Both were decreased -7-fold, while no changes were evident after DNLA treatment. Serine/arginine repetitive matrix 2 (Srrm2) is mislocalized in cytoplasmic lesions of Alzheimer's brain and associated with tauopathy [40]. Srrm2 was decreased -6.5-fold, while no changes after DNLA. G protein signaling modulator 1 (Gpsm1, AGS3) plays roles in G-protein signaling and drug addiction [41]; Nuclear distribution C, dynein complex regulator (Nudc) protein family plays roles in inhibiting the aggregation of several target proteins [42]. Gpsm1 and Nudc were decreased -6.3-fold, while unaltered after DNLA. Myelin basic protein (Mbp) is a marker for myelin damage. In 3 × Tg-AD mouse model, icariin treatment improved the learning and memory, reduced Aβ deposition and tau protein phosphorylation in the hippocampus, while increased myelin-related gene expression including Mbp with reduced myelin damage [43]. Mbp was reduced -6.1-fold, while no change was observed after DNLA. Tau tubulin kinase 1 (Ttbk1) is complexed with microtubule-associated protein tau (MAPT) and is involved in the progression of Alzheimer's disease [44]. The expression of Ttbk1 was decreased -6.1-fold, but attenuated to -4.6-fold by DNLA. Overall, these downregulated protein/genes in SAMP8 mice were prevented or rescued following DNLA treatment.

4.5. Correlation analysis with Alzheimer's disease database

The differentially expressed protein/genes were further correlated with 5 other genomic studies of Alzheimer's disease in the GEO database. Microarray analysis of the astrocyte transcriptome in the aging brain in Alzheimer's patients (GSE29652) [45] generated a -log(p-value) of 3.40 with SAMP8 mice and decreased to 1.07 after 4-month of DNLA treatment; The transcriptome analysis of probable asymptomatic vs symptomatic Alzheimer brains (GSE118553) [46] produced a -log(p-value) of 3.30 with SAMP8 and it was slightly decreased to 3.09 by DNLA; The Superior Temporal Gyrus of patients with definite Alzheimer's disease (GSE84422) [47] generated a -log(p-value) of 3.30 with SAMP8 and decreased to 1.70 after DNLA; A genome-wide gene-expression analysis of transgenic mice during the development of amyloid or tau pathology in the hippocampus revealed that the 72-week old mice (GSE64398) [48] produced a -log(p-value) of 2.85 with SAMP8 and it was decreased to 1.04 by DNLA; However, the 16-week old mice in the same dataset showed negative correlation. Expression of diabetes-related genes in Alzheimer's disease brains in the Hisayama study (GSE 36980) [49] generated a -log(p-value) of 2.70 with SAMP8 and it was decreased to 1.14 after DNLA. Overall, the age-related transcriptome profiles associated with Alzheimer's disease were correlated well with brain proteomics of SAMP8 mice in the present study, and such correlations were attenuated after 4-month of DNLA treatment, supporting the protective role of DNLA to ameliorate age-related changes in SAMP8 mouse hippocampus.

5. Conclusions

This study clearly showed that 4-month of DNLA treatment improved cognitive impairments and neuron damage in aged SAMP8 mice. Phosphorylated proteomic analysis of hippocampal tissues of SAMP8 mice revealed aberrant protein/gene expressions related to several molecular targets and signaling pathways. The 2-dimentional clustering analysis revealed that DNLA ameliorated aberrant protein/gene expression patterns. DNLA prevented or attenuated selected aberrant protein/gene expressions. This proteomic analysis was correlated with the GEO database of genomic changes in Alzheimer's disease and further confirmed beneficial effects of DNLA.

Supplementary Materials: The following supporting information can be downloaded at: https: //www.mdpi.com/article/xxxxxxs1, Supplementary Table S1: 2D-cluster of DEGs.

Author Contributions: Bo Liu: Methodology, Conceptualization, Data curation, Visualization, Writing - original draft; Ling-Li Lv: Data curation, review & editing; Ping Liu: GO and KEGG analysis; Yun-Yan Xu: review & editing; Jie Liu: review & editing, Jing-Shan Shi: funding acquisition, supervision, review & editing, and submit for publication. All authors reviewed and approved the final version of the manuscript.

Funding: This work was supported by the Shi Jing-Shan's Tutor Studio of Pharmacology [GZS-2016(07)]; Funds for the Construction of National First Class Pharmacy Discipline [GESR 2017-85]; Guizhou Science and Technology Department ZK[2022-596]; Research on the Key Technology for High-quality of Dendrobium nobile of Guizhou [K-2019(016)].

Acknowledgements: The authors thank Di Zhao, Jian Sun, Wen-Mei Xiao, Qiong Yang for their help in this study.

Ethic approval: Animal handlings were fully compliance with the Chinese Experimental Animal Guideline, and approved by the Animal Ethics Committee of Zunyi Medical University (ZMU21-2105-002) on May 16, 2021.

Data availability: The data used to support the findings of this study are included within the article.

Declaration of competing interest: All authors declared no conflict of interest.

References

1. Butterfield DA, Poon HF. The senescence-accelerated prone mouse (SAMP8): a model of age-related cognitive decline with relevance to alterations of the gene expression and protein abnormalities in Alzheimer's disease. Exp Gerontol. 2005 Oct;40(10):774-83.
2. Cheng XR, Zhou WX, Zhang YX. The behavioral, pathological and therapeutic features of the senescence-accelerated mouse prone 8 strain as an Alzheimer's disease animal model. Ageing Res Rev. 2014 Jan;13:13-37.
3. Akiguchi I, Pallàs M, Budka H, Akiyama H, Ueno M, Han J, et al. SAMP8 mice as a neuropathological model of accelerated brain aging and dementia: Toshio Takeda's legacy and future directions. Neuropathology. 2017 Aug;37(4):293-305.
4. Liu B, Liu J, Shi JS. SAMP8 Mice as a Model of Age-Related Cognition Decline with Underlying Mechanisms in Alzheimer's Disease. J Alzheimers Dis. 2020;75(2):385-95.
5. Lam Y, Ng TB, Yao RM, Shi J, Xu K, Sze SC, et al. Evaluation of chemical constituents and important mechanism of pharmacological biology in dendrobium plants. Evid Based Complement Alternat Med. 2015;2015:841752.
6. Nie X, Chen Y, Li W, Lu Y. Anti-aging properties of Dendrobium nobile Lindl.: From molecular mechanisms to potential treatments. J Ethnopharmacol. 2020 Jul 15;257:112839.
7. Li DD, Zheng CQ, Zhang F, Shi JS. Potential neuroprotection by Dendrobium nobile Lindl alkaloid in Alzheimer's disease models. Neural Regen Res. 2022 May;17(5):972-77.
8. Nie J, Tian Y, Zhang Y, Lu YL, Li LS, Shi JS. Dendrobium alkaloids prevent Aβ(25-35)-induced neuronal and synaptic loss via promoting neurotrophic factors expression in mice. PeerJ. 2016;4:e2739.
9. Li LS, Lu YL, Nie J, Xu YY, Zhang W, Yang WJ, et al. Dendrobium nobile Lindl alkaloid, a novel autophagy inducer, protects against axonal degeneration induced by Aβ(25-35) in hippocampus neurons in vitro. CNS Neurosci Ther. 2017 Apr;23(4):329-40.
10. Zhang W, Wu Q, Lu YL, Gong QH, Zhang F, Shi JS. Protective effects of Dendrobium nobile Lindl. alkaloids on amyloid beta (25-35)-induced neuronal injury. Neural regeneration research. 2017 Jul;12(7):1131-36.
11. Huang J, Huang N, Zhang M, Nie J, Xu Y, Wu Q, et al. Dendrobium alkaloids decrease Aβ by regulating α- and β-secretases in hippocampal neurons of SD rats. PeerJ. 2019;7:e7627.
12. Nie J, Jiang LS, Zhang Y, Tian Y, Li LS, Lu YL, et al. Dendrobium nobile Lindl. Alkaloids Decreases the Level of Intracellular β-Amyloid by Improving Impaired Autolysosomal Proteolysis in APP/PS1 Mice. Front Pharmacol. 2018;9:1479.
13. Yang S, Gong Q, Wu Q, Li F, Lu Y, Shi J. Alkaloids enriched extract from Dendrobium nobile Lindl. attenuates tau protein hyperphosphorylation and apoptosis induced by lipopolysaccharide in rat brain. Phytomedicine. 2014 Apr 15;21(5):712-6.
14. Liu B, Huang B, Liu J, Shi JS. Dendrobium nobile Lindl alkaloid and metformin ameliorate cognitive dysfunction in senescence-accelerated mice via suppression of endoplasmic reticulum stress. Brain research. 2020 Aug 15;1741:146871.
15. Lv LL, Liu B, Liu J, Li LS, Jin F, Xu YY, et al. Dendrobium nobile Lindl. Alkaloids Ameliorate Cognitive Dysfunction in Senescence Accelerated SAMP8 Mice by Decreasing Amyloid-β Aggregation and Enhancing Autophagy Activity. J Alzheimers Dis. 2020;76(2):657-69.
16. Jin F, Gong QH, Xu YS, Wang LN, Jin H, Li F, et al. Icariin, a phosphodiesterase-5 inhibitor, improves learning and memory in APP/PS1 transgenic mice by stimulation of NO/cGMP signalling. Int J Neuropsychopharmacol. 2014 Jun;17(6):871-81.
17. Seibenhener ML, Wooten MC. Use of the Open Field Maze to measure locomotor and anxiety-like behavior in mice. J Vis Exp. 2015 Feb 6(96):e52434.

18. Chen C, Jiang X, Li Y, Yu H, Li S, Zhang Z, et al. Low-dose oral copper treatment changes the hippocampal phosphoproteomic profile and perturbs mitochondrial function in a mouse model of Alzheimer's disease. Free Radic Biol Med. 2019 May 1;135:144-56.
19. Corton JC, Kleinstreuer NC, Judson RS. Identification of potential endocrine disrupting chemicals using gene expression biomarkers. Toxicol Appl Pharmacol. 2019 Oct 1;380:114683.
20. Su D, Li W, She X, Chen X, Zhai Q, Cui B, et al. Chronic noise exposure exacerbates AD-like neuropathology in SAMP8 mice in relation to Wnt signaling in the PFC and hippocampus. Sci Rep. 2018 Oct 2;8(1):14622.
21. Hansen HH, Fabricius K, Barkholt P, Niehoff ML, Morley JE, Jelsing J, et al. The GLP-1 Receptor Agonist Liraglutide Improves Memory Function and Increases Hippocampal CA1 Neuronal Numbers in a Senescence-Accelerated Mouse Model of Alzheimer's Disease. J Alzheimers Dis. 2015;46(4):877-88.
22. Xiong TW, Liu B, Wu Q, Xu YY, Liu P, Wang Y, et al. Beneficial effects of Dendrobium nobile Lindl. Alkaloids (DNLA) on anxiety and depression induced by chronic unpredictable stress in rats. Brain Res. 2021 Nov 15;1771:147647.
23. Cheng XR, Cui XL, Zheng Y, Zhang GR, Li P, Huang H, et al. Nodes and biological processes identified on the basis of network analysis in the brain of the senescence accelerated mice as an Alzheimer's disease animal model. Front Aging Neurosci. 2013;5:65.
24. Wendler F, Purice TM, Simon T, Stebbing J, Giamas G. The LMTK-family of kinases: Emerging important players in cell physiology and pathogenesis. Biochim Biophys Acta Mol Basis Dis. 2021 Sep 1;1867(9):165372.
25. Piatnitskaia S, Takahashi M, Kitaura H, Katsuragi Y, Kakihana T, Zhang L, et al. USP10 is a critical factor for Tau-positive stress granule formation in neuronal cells. Sci Rep. 2019 Jul 22;9(1):10591.
26. Lang M, Wang L, Fan Q, Xiao G, Wang X, Zhong Y, et al. Genetic inhibition of solute-linked carrier 39 family transporter 1 ameliorates aβ pathology in a Drosophila model of Alzheimer's disease. PLoS Genet. 2012;8(4):e1002683.
27. Poirier K, Hubert L, Viot G, Rio M, Billuart P, Besmond C, et al. CSNK2B splice site mutations in patients cause intellectual disability with or without myoclonic epilepsy. Hum Mutat. 2017 Aug;38(8):932-41.
28. Shi Q, Ge Y, He W, Hu X, Yan R. RTN1 and RTN3 protein are differentially associated with senile plaques in Alzheimer's brains. Sci Rep. 2017 Jul 21;7(1):6145.
29. Saetre P, Jazin E, Emilsson L. Age-related changes in gene expression are accelerated in Alzheimer's disease. Synapse. 2011 Sep;65(9):971-4.
30. King CR, AR AAQ, Chazeau A, Saarloos I, van der Graaf AJ, Verhage M, et al. Fbxo41 Promotes Disassembly of Neuronal Primary Cilia. Sci Rep. 2019 Jun 3;9(1):8179.
31. Lin L, Lyu Q, Kwan PY, Zhao J, Fan R, Chai A, et al. The epilepsy and intellectual disability-associated protein TBC1D24 regulates the maintenance of excitatory synapses and animal behaviors. PLoS Genet. 2020 Jan;16(1):e1008587.
32. Regan P, Mitchell SJ, Kim SC, Lee Y, Yi JH, Barbati SA, et al. Regulation of Synapse Weakening through Interactions of the Microtubule Associated Protein Tau with PACSIN1. J Neurosci. 2021 Aug 25;41(34):7162-70.
33. Pérez-Villegas EM, Pérez-Rodríguez M, Negrete-Díaz JV, Ruiz R, Rosa JL, de Toledo GA, et al. HERC1 Ubiquitin Ligase Is Required for Hippocampal Learning and Memory. Front Neuroanat. 2020;14:592797.
34. Yu Y, Li Y, Zhang Y. Yeast Two-Hybrid Screening for Proteins that Interact with the Extracellular Domain of Amyloid Precursor Protein. Neurosci Bull. 2016 Apr;32(2):171-6.
35. Quan X, Liang H, Chen Y, Qin Q, Wei Y, Liang Z. Related Network and Differential Expression Analyses Identify Nuclear Genes and Pathways in the Hippocampus of Alzheimer Disease. Med Sci Monit. 2020 Jan 28;26:e919311.
36. Hondius DC, van Nierop P, Li KW, Hoozemans JJ, van der Schors RC, van Haastert ES, et al. Profiling the human hippocampal proteome at all pathologic stages of Alzheimer's disease. Alzheimers Dement. 2016 Jun;12(6):654-68.
37. Key J, Harter PN, Sen NE, Gradhand E, Auburger G, Gispert S. Mid-Gestation lethality of Atxn2l-Ablated Mice. Int J Mol Sci. 2020 Jul 20;21(14).
38. Kondo M, Takei Y, Hirokawa N. Motor protein KIF1A is essential for hippocampal synaptogenesis and learning enhancement in an enriched environment. Neuron. 2012 Feb 23;73(4):743-57.
39. Lee KH, Lee JS, Lee D, Seog DH, Lytton J, Ho WK, et al. KIF21A-mediated axonal transport and selective endocytosis underlie the polarized targeting of NCKX2. J Neurosci. 2012 Mar 21;32(12):4102-17.
40. McMillan PJ, Strovas TJ, Baum M, Mitchell BK, Eck RJ, Hendricks N, et al. Pathological tau drives ectopic nuclear speckle scaffold protein SRRM2 accumulation in neuron cytoplasm in Alzheimer's disease. Acta Neuropathol Commun. 2021 Jun 29;9(1):117.
41. Bowers MS. Activators of G-protein signaling 3: a drug addiction molecular gateway. Behav Pharmacol. 2010 Sep;21(5-6):500-13.
42. Zheng M, Cierpicki T, Burdette AJ, Utepbergenov D, Janczyk P, Derewenda U, et al. Structural features and chaperone activity of the NudC protein family. J Mol Biol. 2011 Jun 24;409(5):722-41.
43. Yu H, Shi J, Lin Y, Zhang Y, Luo Q, Huang S, et al. Icariin Ameliorates Alzheimer's Disease Pathology by Alleviating Myelin Injury in 3 × Tg-AD Mice. Neurochem Res. 2022 Jan 17.
44. Yan Y, Yan H, Teng Y, Wang Q, Yang P, Zhang L, et al. Long non-coding RNA 00507/miRNA-181c-5p/TTBK1/MAPT axis regulates tau hyperphosphorylation in Alzheimer's disease. J Gene Med. 2020 Dec;22(12):e3268.
45. Simpson JE, Ince PG, Shaw PJ, Heath PR, Raman R, Garwood CJ, et al. Microarray analysis of the astrocyte transcriptome in the aging brain: relationship to Alzheimer's pathology and APOE genotype. Neurobiol Aging. 2011 Oct;32(10):1795-807.
46. Patel H, Hodges AK, Curtis C, Lee SH, Troakes C, Dobson RJB, et al. Transcriptomic analysis of probable asymptomatic and symptomatic alzheimer brains. Brain Behav Immun. 2019 Aug;80:644-56.

 doi:10.20944/preprints202212.0313.v1

47. Wang M, Roussos P, McKenzie A, Zhou X, Kajiwara Y, Brennand KJ, et al. Integrative network analysis of nineteen brain regions identifies molecular signatures and networks underlying selective regional vulnerability to Alzheimer's disease. Genome Med. 2016 Nov 1;8(1):104.
48. Matarin M, Salih DA, Yasvoina M, Cummings DM, Guelfi S, Liu W, et al. A genome-wide gene-expression analysis and database in transgenic mice during development of amyloid or tau pathology. Cell Rep. 2015 Feb 3;10(4):633-44.
49. Hokama M, Oka S, Leon J, Ninomiya T, Honda H, Sasaki K, et al. Altered expression of diabetes-related genes in Alzheimer's disease brains: the Hisayama study. Cereb Cortex. 2014 Sep;24(9):2476-88.